

Bioinorganic Chemistry of Bismuth and Antimony: Target Sites of Metallodrugs

RUIGUANG GE AND HONGZHE SUN*

Department of Chemistry and Open Laboratory of Chemical Biology, The University of Hong Kong, Pokfulam, Hong Kong, P. R. China

Received October 18, 2006

ABSTRACT

The biocoordination chemistry of antimony and bismuth has been extensively investigated due to the historical use of these metals in medicine. Structures of bismuth antiulcer agents and interactions of Bi^{3+} with proteins and enzymes, such as transferrin and lactoferrin, the histidine-rich protein Hpn, and urease, have been characterized. Sb^{5+} is a prodrug and is bioreduced or activated to its active form Sb^{3+} intracellularly. Antimony binds to biomolecules, such as glutathione, trypanothione, and nucleotides, and forms binary and ternary complexes, which may allow it to be trafficked in cells. These studies have improved our understanding of the mechanism of action of bismuth and antimony drugs, which in turn allows the future design of drugs.

1. Introduction

Both antimony and bismuth belong to the same group in the periodic table, together with nitrogen, phosphorus, and arsenic. Bismuth compounds have been used in medicine for more than two centuries for the treatment of *Helicobacter pylori* infection and other gastrointestinal disorders.^{1,2} Antimony-containing compounds are commonly used to treat parasitic infections such as leishmaniasis, but drug resistance and side effects associated with the use of these antimony compounds have aroused concern.³ This Account briefly summarizes recent progress on the structures of group 15 metallodrugs and their interactions with proteins and enzymes, which are of fundamental importance in understanding their biological activities at the molecular level.

2. Structure

Structures of Bismuth Subsalsicylate (BSS) and Bismuth Citrate. Bi^{3+} is highly acidic in water ($\text{p}K_{\text{a}1}$ of ca. 1.5) and has a strong tendency to form stable hydroxo- and oxo-bridged clusters. Dimeric and polymeric structures are commonly observed for bismuth complexes resulting from the ligand engaging more than one Bi^{3+} center and

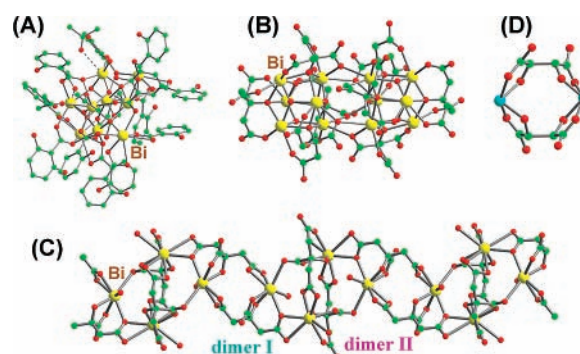


FIGURE 1. Structures of bismuth and antimony drugs: (A) the octahedral arrangement of the Bi atoms in $[\text{Bi}_9\text{O}_7(\text{Hsal})_{13}(\text{Me}_2\text{CO})_5]$ with seven octahedral faces capped by an oxygen atom; (B) structure of the dodecanuclear oxo-citrate bismuth cluster unit $[\text{Bi}_{12}\text{O}_8(\text{cit})_8]^{12-}$; (C) the polyanionic chain of $[\text{Bi}(\text{cit})_2\text{Bi}]_2^{2-}$ aggregated from dimers I and II under acidic conditions; (D) dimeric structure of Sb^{3+} tartrate. Color code: Bi, yellow; O, red; C, green; Sb, sky blue.

behaving as a bridging ligand (e.g., O^{2-} , citrate), Figure 1A–C. The coordination number of Bi^{3+} is highly variable (from 3 to 10), and the coordination geometry is often irregular.⁴

Although bismuth subsalsicylate (BSS), colloidal bismuth citrate (CBS), and ranitidine bismuth citrate (RBC) have been used as antiulcer drugs for decades, their structures have only recently been reported. Several bismuth subsalsicylate complexes have been synthesized and structurally characterized by X-ray crystallography very recently.⁵ Salsicylate ligands are coordinated to all bismuth atoms via chelation, with extraordinary variations in binding modes. The Bi_9 clusters in both $[\text{Bi}_9\text{O}_7(\text{Hsal})_{13}(\text{Me}_2\text{CO})_5] \cdot (\text{Me}_2\text{CO})_{1.5}$ (Figure 1A) and $[\text{Bi}_{38}\text{O}_{44}(\text{Hsal})_{26}(\text{Me}_2\text{CO})_{15} \cdot (\text{H}_2\text{O})_2] \cdot (\text{Me}_2\text{CO})_4$ comprise a central Bi_6 octahedron ($[\text{Bi}_6\text{O}_8]^{2+}$), a common building block of bismuth-oxo compounds. Very short bonds in the oxide core (2.06–2.09 Å) and medium and long bonds resulting from asymmetric coordination of the carboxylate groups are found in these structures, with the coordination numbers for bismuth being either six, seven, or eight.⁴ The Bi_9 cluster may aggregate to form Bi_{38} clusters. Although stable in organic solvents, these complexes may slowly hydrolyze in aqueous solution to form a mixture of clusters, which accounts for the poor solubility of BSS.

In contrast to BSS, both CBS and RBC are highly water soluble, and their solubilities are dependent on pH and ionic strength, ranging from around 1 g/mL in pure water to 1 mg/mL at acidic pH and high ionic strength (e.g., in the stomach). They have been commonly used for the treatment of peptic ulcers and *H. pylori* infections, together with antibiotics, which has stimulated extensive structural studies of bismuth complexes with (sub)citrate. The empirical formula of CBS was previously reported as $\text{K}_3(\text{NH}_4)_2[\text{Bi}_6\text{O}_3(\text{OH})_5(\text{Hcit})_4]$ in the Merck Index but has

* To whom correspondence should be addressed. Tel: (852) 2859-8974. Fax: (852) 2857-1586, E-mail: hsun@hkucc.hku.hk.

Ruiguang Ge received his B.Sc. and M.Sc. in 1999 and 2002 from China University of Petroleum and Nankai University, respectively. He is working toward a Ph.D. in Chemistry at the University of Hong Kong. His current research interest is the bioinorganic chemistry of nickel.

Hongzhe Sun received his Ph.D from the University of London in 1996. After postdoctoral work at University of Edinburgh, he joined the faculty of the University of Hong Kong in 1998 where he is currently an Associate Professor. His research interests are the biological chemistry of metallodrugs and metalloproteins.

been revised to a less precise formula in the latest edition to reflect its complicated polymeric nature.⁶

By variation of the pH and the ratios of Bi^{3+} and citrate, about ten different bismuth citrate complexes have been obtained and characterized by X-ray crystallography. The majority of these contain a complex of Bi^{3+} with a tridentate citrate, which forms a stable dinuclear unit $[\text{Bi}(\text{cit})_2\text{Bi}]^{2-}$, with additional OH^- , O^{2-} , and H_2O ligands. These complexes are also characterized by a short Bi–O (alkoxide) bond (*ca.* 2.2 Å) and stereochemically lone pairs of electrons from the Bi^{3+} . At neutral pH, both multinuclear clusters and linear polymers are present through citrate and oxo bridging. The dodecanuclear oxo-citrate bismuth cluster $[\text{Bi}_{12}\text{O}_8(\text{cit})_8]^{12-}$ unit (Figure 1B), which has a symmetry of inversion, is composed of two $[\text{Bi}_6\text{O}_4(\text{cit})_4]^{6-}$ cluster units.⁷ The structure of $[\text{Bi}_6\text{O}_4(\text{cit})_4]^{6-}$ is comparable to that of $[\text{Bi}_6\text{O}_4(\text{OH})_4]^{6+}$, in which the four hydroxides are substituted by the hydroxyl oxygen from each citrate. Both clusters have almost an identical Bi_6O_8 core, a common basic building block found in bismuth-oxo compounds. The Bi_{12} cluster can further aggregate to form a mixture of $(\text{Bi}_{12})_n$ ($n = 1, 2, \dots$) species in concentrated solutions and upon dilution may dissociate or undergo hydrolytic decomposition to form smaller clusters such as $[\text{Bi}_6\text{O}_4(\text{cit})_4]^{6-}$ with the release of some citrate.

Structural studies of bismuth citrate under acidic conditions (e.g., $\text{pH} \approx 3$) were made to understand the possible pharmacokinetics as well as the composition of the CBS and RBC species that may be present in the stomach. These revealed that only linear polyanionic complexes were obtained (Figure 1C).^{8,9} Interestingly, three types of bismuth citrate dinuclear unit $[\text{Bi}(\text{cit})_2\text{Bi}]^{2-}$ were present with Bi...Bi distances ranging from 5.74 to 6.08 Å. In these dimers, each Bi^{3+} is coordinated to three oxygens from one citrate in a tridentate mode as well as a doubly bridged terminal carboxylate group from another citrate in the form of a four-membered chelate. The coordination of each bismuth in one dimer (I) is complemented by a monodentate oxygen from a citrate belonging to the adjacent dimer (II) (Bi–O, 2.79 Å) and one water molecule (Bi–O, 2.45 Å). The coordination numbers for the Bi^{3+} centers in these dimers are seven and eight, respectively. Unlike the arrangement found in other Bi^{3+} -citrate complexes, dimer II is vertically inserted between two adjacent structural units (I). The assembly formed by dimers I and II leads to the formation of not only a “tetrameric unit” and subsequently a “linear polyanionic chain” but also a two-dimensional network (sheet) and 3D structures, forming a large mesh with channels via further cross-linking. In solution, the interconversion of different bismuth citrate species can be observed by NMR. Ligand exchange rates are relatively slow on the NMR time scale at $\text{pH} > 6.2$ but become much faster at $\text{pH} < 5$. When the pH is varied from neutral to acidic pH values, CBS may rearrange from clusters such as $[\text{Bi}_6\text{O}_6(\text{cit})_4]^{6-}$ and $[\text{Bi}_{12}\text{O}_8(\text{cit})_8]^{12-}$ and linear polymer anions $[\text{Bi}(\text{cit})_2\text{Bi}]_{\infty}^{2n-}$, to sheets and 3D polymers (e.g., $[\text{Bi}(\text{cit})_2\text{Bi}]_{\infty}^{2n-}$ or $[\text{Bi}(\text{cit})_2(\text{Hcit})\text{Bi}]_{\infty}^{5n-}$) due to rapid ligand exchange. RBC may adopt a similar bismuth citrate skeleton ($[\text{Bi}(\text{cit})_2-$

$\text{Bi}]_{\infty}^{2n-}$) based on their similarities in chemical compositions (Bi/cit = 1:1) and crystallization conditions (pH 3–4).⁹ These polymeric anions formed by sheets and chains could be the potential “active species” of the antiulcer drugs in the stomach and may be selectively deposited on the ulcerous craters to form a “protective coating”. Cleavage of the doubly bridged carboxylates between the dimers by either citrate or water would lead to singly bridged polyanionic species and to other low molecular weight bismuth citrate species, which would allow the metal to be taken-up by bacteria. The interaction of these polymers with membrane surfaces may be important to their bioactivity and bioavailability.

Using the linear polymeric $[\text{Bi}(\text{cit})_2\text{Bi}]_{\infty}^{2n-}$ chain as a template, bismuth subcarbonate nanotubes with a diameter of 4.0 ± 0.5 nm have been prepared. Notably, these nanotubes exhibited slightly higher antibacterial activities ($\text{IC}_{50} = 10 \mu\text{g}/\text{mL}$) against *H. pylori* than CBS¹⁰ and may provide a structural basis for the design and development of future bismuth nanomedicines.

Antimony Structures. Sb^{5+} -containing compounds, such as sodium stibogluconate (Pentostam) and meglumine antimonate (Glucantime), have been used clinically against different forms of leishmaniasis. They are more effective and 10-fold less toxic than their trivalent analogues, although Sb^{5+} is generally regarded as a pro-drug, which is reduced or activated into Sb^{3+} *in vivo*.¹¹ The precise molecular structures of stibogluconate and meglumine antimonate have not been unambiguously determined. It is commonly believed that the former is a mixture of Sb^{5+} and carbohydrate with apparent molecular masses ranging from 746 (probably corresponding to a dimer) to 4 kDa (polymeric species). The major species of meglumine antimonate in aqueous solution is $\text{Sb}(\text{NMG})_2$ (where NMG = *N*-methyl-D-glucamine) with a formula mass of 507. However, a series of oligomers of Sb^{5+} and *N*-methyl-D-glucamine have also been observed with the general formula $\text{Sb}_n(\text{NMG})_{n+1}$ or $\text{Sb}_n(\text{NMG})_n$ ($n = 1-4$),¹² which exist in equilibrium in solution.

The clinically used trivalent antimony agent, potassium antimony(III) tartrate, is a dimer.¹³ Each antimony coordinates in a bidentate mode to four oxygens from each of the two tartrate ligands (Figure 1D). The coordination geometry of Sb^{3+} is distorted pseudo-trigonal bipyramidal. In solution, both monomers and dimers exist in equilibrium with monomers being the major species at higher pH values.

3. Interactions of Antimony and Bismuth Compounds with Biomolecules

Bismuth Binding to Proteins. Transferrin comprises a family of large (~80 kDa) non-heme glycoproteins with the principal biological function of ferric iron binding and transportation (with the exception of melanotransferrin).¹⁴ Serum transferrin has the role of carrying Fe^{3+} from the site of intake into the blood plasma and tissues by endocytosis of the diferric protein in association with transferrin receptor. It is also likely to be involved in the

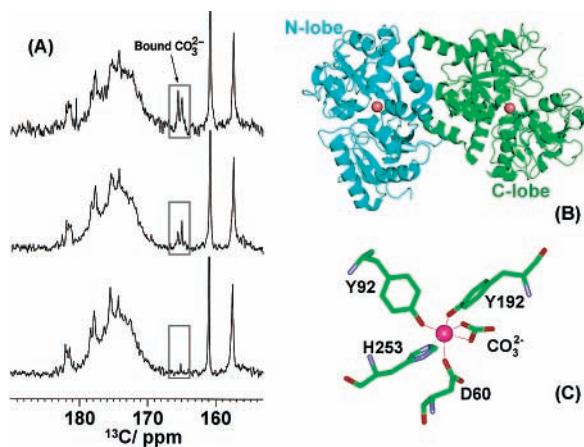


FIGURE 2. (A) 125 MHz ^{13}C NMR spectra of hLF (1.2 mM, 50% H_2O , $\text{pH}^* 7.4$) in the presence of 10 mM $\text{H}^{13}\text{CO}_3^-$ with the addition of 0, 1, or 2 molar equiv of $\text{Bi}(\text{NTA})$ (from bottom to top), (B) X-ray structure of the Fe_2 -hLF (PDBID, 1B0L) with the two lobes labeled as N- and C-lobes and the Fe^{3+} ions (as balls) highlighted, and (C) the Fe^{3+} binding site in the N-lobe of lactoferrin. Adapted from ref 17.

delivery of other metal ions including therapeutic, radio-diagnostic, and toxic ions.¹⁵ The strength of metal binding to transferrin was found to simply correlate with the metal acidity. A related protein, lactoferrin, is believed to serve mainly as a bacteriostat by chelating iron, a metal essentially required for the growth of microorganisms. Lactoferrin binds Fe^{3+} with an affinity 100-fold higher than that of transferrin.¹⁶ However the rates of uptake and release of the metal by lactoferrin are much lower than for those of transferrin.¹⁴

Bi^{3+} binds strongly to the iron binding sites of human transferrin (hTF) and lactoferrin (hLF), both in the N- and C-lobes, along with either carbonate or oxalate as the synergistic anion.^{17,18} Our NMR data suggest that binding of Bi^{3+} occurs preferentially in the C-lobe of transferrin. In contrast, there is no site preference for the binding of Bi^{3+} to human lactoferrin, as demonstrated by the simultaneous increase in the intensity of the bound carbonate signals at 165.9 and 165.2 ppm, Figure 2. The relatively large difference in chemical shifts indicates that the two bound carbonates in lactoferrin are in slightly different environments in each of the two lobes, in contrast to what is found in human transferrin. Similar to Fe^{3+} , the binding of Bi^{3+} to human lactoferrin is reversible with a half-dissociation pH ($\text{pH}_{1/2}$) of 5.2. Significantly, the Bi_2 -hLF complex blocks the uptake of $^{59}\text{Fe}_2$ -hLF into rat IEC-6 cells, indicating that Bi^{3+} -loaded lactoferrin is recognized by the protein receptor and can be taken-up into the cells via a “receptor-mediated endocytosis” process.¹⁷ Since lactoferrin is known to be present in significant amounts in the stomach secretions of patients with gastritis, Bi^{3+} may therefore interfere with iron metabolism in bacteria. The accumulated intracellular Bi^{3+} may then interact with proteins and enzymes in bacteria.

The neurotoxicity associated with the use of bismuth drugs is generally diagnosed by the detection of bismuth in blood, plasma, or serum.¹⁹ In blood, bismuth is thought to be primarily present in the red blood cells, with the

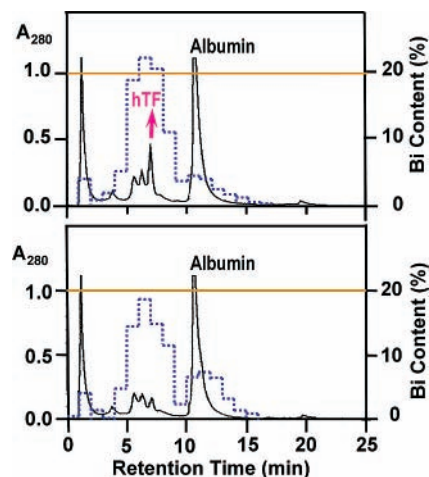


FIGURE 3. Distribution of Bi^{3+} among components of normal human serum (bottom) and human serum in the presence of elevated transferrin (top). The solid line and dotted lines represent the chromatogram of human serum separation by an anion-exchange column and bismuth profile (%). Adapted from ref 21.

remaining portion found in serum and plasma.²⁰ The binding of Bi^{3+} to serum transferrin in the presence of a large excess of albumin and even in blood plasma itself can be directly monitored by NMR using isotopically labeled protein. Bi^{3+} binds to transferrin even in the presence of a 10-fold excess of serum albumin. This occurs despite the presence of a free thiolate group at Cys34, which would be expected to have a higher affinity for Bi^{3+} than oxygen and nitrogen ligands.¹⁸ This clearly suggests that the accessibility of the potential target site(s) for metallodrugs (e.g., Bi^{3+}) is of key importance. The Bi^{3+} -induced changes in shifts of the $^1\text{H}/^{13}\text{C}$ resonances of the labeled transferrin are similar to those induced by Ga^{3+} and Fe^{3+} , suggesting that there are similar conformational changes.

In agreement with the NMR study, competitive binding studies between Bi^{3+} and human albumin and transferrin monitored by fast protein liquid chromatography (FPLC) and inductively coupled plasma mass spectrometry (ICP-MS) showed that $>70\%$ of bismuth is associated with transferrin even in the presence of 13 molar equiv of albumin (Figure 3).²¹ Bismuth was found to bind to albumin only when iron-saturated transferrin was used. Therefore, transferrin is probably the major transporter of Bi^{3+} in blood plasma, indicating that it plays an important role in the pharmacology of bismuth.

Bi^{3+} Inhibition of Enzymes. Pathogenic microorganisms such as *H. pylori* produce large amounts of enzymes, and enzyme inhibition has long been thought to play a critical role in the activities of bismuth antiulcer drugs. It has previously been demonstrated that bismuth drugs inhibit several enzymes from *H. pylori*, for example, cytosolic alcohol dehydrogenase (ADH),²² ATPase, and urease.²³ The zinc-containing enzyme ADH is responsible for the oxidation of alcohols to acetaldehydes, which are toxic to mucosal cells. Kinetic analyses have shown that Bi^{3+} (as CBS) acts as a noncompetitive inhibitor of yeast alcohol dehydrogenase. Bi^{3+} binds to thiolate groups on

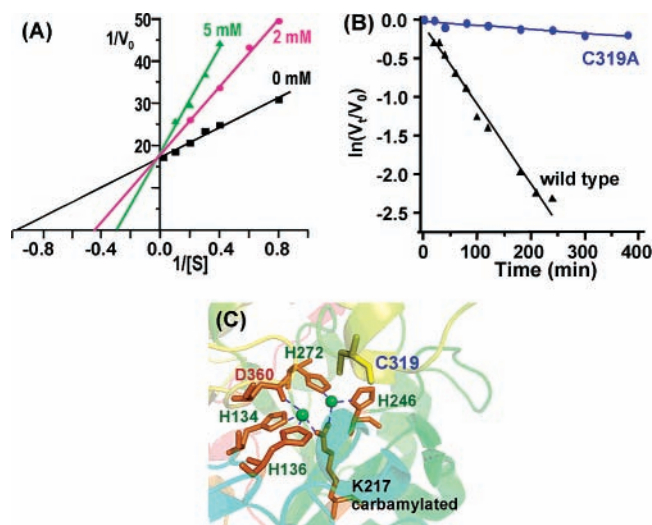


FIGURE 4. *K. aerogenes* urease inhibition by Bi(EDTA): (A) double reciprocal plots of wild-type *K. aerogenes* urease inhibition by Bi(EDTA); (B) kinetics of the inhibition of the wild-type and active C319A mutant *K. aerogenes* urease by 2 mM Bi(EDTA) in 50 mM Hepes at pH 7.0; (C) the active site of the enzyme with the cysteine highlighted. Adapted from ref 26.

the enzyme as evidenced by the increase in absorbance at 350 nm upon addition of Bi^{3+} .²⁴ The interaction between Bi^{3+} and the enzyme exhibits biphasic behavior, and only one of the two Zn^{2+} ions can be substituted by Bi^{3+} . Since the inhibition is noncompetitive, it likely replaces the Zn^{2+} at the structural site, which is coordinated to four cysteine residues. Interestingly, the binding of Bi^{3+} to the enzyme gradually promotes enzyme multimer dissociation, favoring the formation of a dimer, rather than its native tetrameric arrangement.²⁴

Urease in *H. pylori* is essentially required for colonization of the gastric mucus and for the survival of the bacterium under highly acidic conditions. It catalyzes the hydrolysis of urea to ammonia and carbon dioxide, which helps to maintain the periplasmic pH value at ca. 6.2. Urease has long been regarded as a potential target for antiulcer drug design. Bismuth complexes are found to efficiently inhibit the enzyme.²⁵ Since ureases have highly conserved sequences, the three-dimensional structures and the active site (dinuclear nickel center), the inhibition of Jack bean urease by various bismuth complexes has been investigated. RBC has been shown to act as a noncompetitive inhibitor with a K_i value of 1.17 mM, while Bi(EDTA) and Bi(Cys)₃ are competitive inhibitors with similar K_i values to RBC.²⁶ The decrease in free thiolates by 12 and 6 per hexamer (i.e., 2 and 1 per monomer) upon incubation of Jack bean urease with RBC and Bi(EDTA), respectively, suggested that Bi^{3+} ions are possibly bound to exposed cysteine residues on the enzyme. Bi^{3+} (as Bi(EDTA)) reversibly inhibited the urease from *Klebsiella aerogenes*. Incubation of the wild-type enzyme with Bi^{3+} led to a first-order decrease in enzyme activity (Figure 4). The significant decrease in the rate of inactivation of the catalytically active C319A mutant of the bacterial enzyme ($5.04 \times 10^{-4} \text{ min}^{-1}$) under identical conditions, as compared with the wild type ($9.95 \times 10^{-3} \text{ min}^{-1}$), clearly

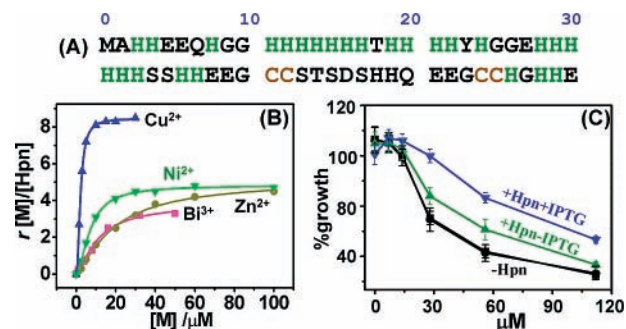


FIGURE 5. Hpn, a nickel-storage protein in *H. pylori*: (A) amino acid sequence of Hpn with the histidine residues and cysteine pairs highlighted; (B) Hpn binds to Cu^{2+} , Ni^{2+} , Zn^{2+} , and Bi^{3+} ; (C) Hpn protects *E. coli* cells from the extracellular Bi^{3+} ions.

indicated that urease inactivation is mainly due to the interaction of Bi^{3+} with Cys319 (Figure 4B,C). This residue is conserved in ureases from several species and is located on a flap at the entrance to the active site. Binding of Bi^{3+} to this residue may seal the entrance to the active cavity.

Nickel is important for the survival of *H. pylori*, and a constant supply of nickel ions is required for the synthesis and activity of the urease and hydrogenase. However, high concentrations of nickel ions are toxic. *H. pylori* synthesizes an unusual histidine-rich cytoplasmic protein (28 histidines out of 60 aa), Hpn, which may play a role in the storage of nickel ions and shares some similarities to the $\text{Zn}^{2+}/\text{Cu}^+$ storage protein metallothionein. The transcriptional synthesis of Hpn is upregulated by the nickel regulatory protein (NikR) in the presence of excess of nickel. *H. pylori* strains containing an *hpn* knock-out gene are 4-fold more susceptible to Ni^{2+} and Bi^{3+} than the wild-type strain, indicating a potential role of the protein in alleviating the toxicity by sequestering excess intracellular metals. Hpn exists as a multimer, with a 20-mer being the predominant species in solution. It binds around $4.8 \pm 0.2 \text{ Ni}^{2+}$ and $3.8 \pm 0.2 \text{ Bi}^{3+}$ ions per monomer with moderate strength (K_d of 7.1 and 11.1 μM , respectively), Figure 5.^{27,28} Importantly, Ni^{2+} binding is reversible: the metal being released from the protein either in the presence of a chelating ligand such as EDTA or at a slightly acidic pH ($\text{pH}_{1/2} \approx 6.3$). At $[\text{Bi}^{3+}] > 30 \mu\text{M}$, *Escherichia coli* BL21 cells with the *hpn* gene on a pET plasmid were found to grow slightly better upon addition of isopropyl- β -D-thiogalactopyranoside (IPTG) than those without, and cells without the *hpn* gene grew much slowly than those with *hpn*, Figure 5C. Strains with and without *hpn* similarly exhibited different growth rates in the presence of Ni^{2+} . In contrast, comparable cell growth was observed in the presence of Cu^{2+} and Zn^{2+} . This suggests that Hpn may be involved in nickel storage and homeostasis.

Sb^{5+} Binding to Nucleotides. Both Sb^{5+} and Sb^{3+} have been shown to form complexes with the ribose moiety of nucleotides.^{29,30} Combined with the fact that Sb^{5+} undergoes a relatively slow reduction in parasites, this indicates that the formation of antimony–nucleotide complexes is possible *in vivo*. Sb^{5+} forms relatively stable 1:1, 1:2, and 1:3 complexes with nucleotides containing vicinal *cis*-hydroxyl groups (e.g., adenosine, cytidine, guanosine,

uridine, and AMP) under physiological conditions.³¹ Stable mono- and bisadducts of Sb^{5+} are formed with guanosine 5'-monophosphate (5'-GMP) and guanosine 5'-diphospho-D-mannose through binding to the deprotonated hydroxyl group ($-\text{O}^-$) of the ribose moiety, with the monoadduct kinetically and thermodynamically favored.³² Oxygen atoms from water molecules may be involved in complex formation. The rate of formation of the monoadducts ($\text{Sb}(5'\text{-GMP})$ and $\text{Sb}(5'\text{-GDP-mannose})$) is 10-fold faster than that of the bisadducts ($\text{Sb}(5'\text{-GMP})_2$ and $\text{Sb}(5'\text{-GDP-mannose})_2$). The preferential formation of monoadducts suggests that the nucleotides may act as carriers mediating the transport of Sb^{5+} into parasites, for example, via the lipophosphoglycan (LPG) transporter.

Reduction or Activation of Pentavalent Antimony. As noted above, it has long been thought that Sb^{5+} is a prodrug and is bioreduced to Sb^{3+} , the active form of the drug.³³ Reduction occurs preferentially in amastigotes, which are more sensitive to stibogluconate than promastigotes.

Low molecular weight (LMW) thiols such as glutathione have been shown to reduce Sb^{5+} .³⁴ However, this process is too slow to be biologically significant. Rather than glutathione, trypanothione ($\text{T}(\text{SH})_2$) is the most important LMW thiol inside *Leishmania* species and is involved in the maintenance of cellular redox homeostasis together with trypanothione reductase.³⁵ Surprisingly, $\text{T}(\text{SH})_2$ has been found to rapidly reduce Sb^{5+} to Sb^{3+} , particularly under acidic conditions and at slightly elevated temperature ($k = 4.42 \text{ M}^{-1} \text{ min}^{-1}$ at pH 6.4, 310 K).^{36,37} Because amastigotes have a lower intracellular pH and a higher temperature, the rapid reduction of Sb^{5+} by the $\text{T}(\text{SH})_2$ is more favorable in amastigotes compared with promastigotes. However, the physiological relevance of this observation required further analysis because promastigotes contain higher intracellular concentrations of $\text{T}(\text{SH})_2$ and GSH than amastigotes;³⁸ intracellular pH values are maintained at pH values close to neutral and are independent of external pH during both stages.³⁹ Both can take up Sb^{5+} and Sb^{3+} .⁴⁰

To date, two enzymes have been found to be able to catalyze the reduction of Sb^{5+} to Sb^{3+} . *LmACR2*, from *Leishmania major*, is the first identified metalloid reductase with a physiological role in drug activation.⁴¹ It is able to reduce both arsenate (As^{5+}) and antimonate (Sb^{5+}) but is more efficient at reducing antimonate, with a reduction rate of around 33 and 10 $\text{nmol}\cdot\text{mg}^{-1}\cdot\text{min}^{-1}$ for Sb^{5+} and As^{5+} , respectively, in the presence of glutaredoxin and GSH.

Another enzyme that is possibly involved in Sb^{5+} reduction is a thiol-dependent reductase (TDR1) that uses glutathione as the reductant.⁴² The reduction rates for stibogluconate and meglumine antimonite are 6.3 and 1.4 $\mu\text{M}\cdot\text{min}^{-1}$, respectively. Expression of TDR1 in amastigotes is around 10-fold higher than that in promastigotes, which may explain the higher sensitivity of amastigotes to Sb^{5+} -based antimonials compared with promastigotes. However, this does not exclude additional reductions by the host macrophage.

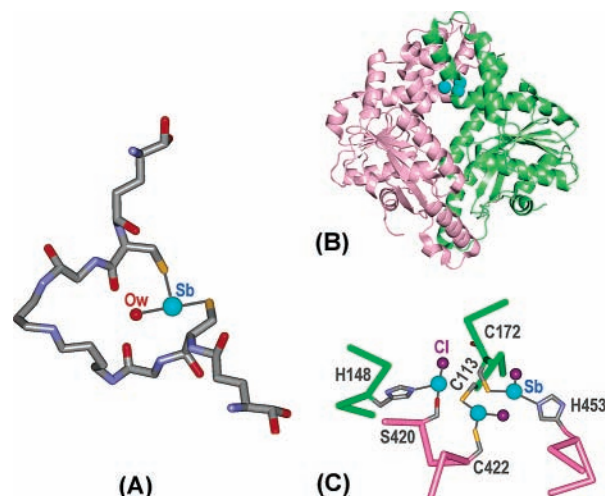


FIGURE 6. (A) Solution structure of $\text{SbT}(\text{S})_2$ with a bound water molecule noted, (B) overall structure of the ArsA ATPase with the novel trinuclear Sb^{3+} cluster highlighted (PDBID, 1F48), and (C) coordination of Sb^{3+} at the active site. Each metal is bound to two residues from the protein and one chloride—C172 and H453, H148 and S420, and C113 and C422. Adapted from refs 44 and 45. The sky blue and purple balls represent Sb^{3+} and Cl^- , respectively.

Interaction of Sb^{3+} with $\text{T}(\text{SH})_2$ and ArsA. Both arsenic and antimony are classified as semimetals. The trivalent antimony is a borderline metal ion and has a high affinity toward thiolate sulfur-, oxygen- and nitrogen-containing ligands. Its antileishmanial action is likely to be related to its interaction with thiolate- and nitrogen-containing proteins and enzymes. Sb^{3+} forms stable complexes with glutathione and trypanothione with a stoichiometry of $\text{Sb}(\text{TS}_2)$ and $\text{Sb}(\text{GS})_3$.⁴³ Spin-echo NMR studies have shown that the uptake of Sb^{3+} (as potassium antimony tartrate) into red cells and its complexation with the intracellular glutathione occurs rapidly ($t_{1/2}$ of minutes). Due to the presence of two isotopes with similar natural abundance ($^{121}\text{Sb}/^{123}\text{Sb} = 57.25:42.75$), characteristic peaks can be observed in electrospray ionization (ESI)-MS spectra upon antimony binding to biomolecules (Figure 7). Strong binding of Sb^{3+} to trypanothione was examined by NMR and ESI-MS, together with FPLC. Surprisingly, a $\text{Sb}(\text{TS}_2)$ complex was formed with the Sb^{3+} binding affinity being 100-fold higher than that in $\text{Sb}(\text{GS})_3$ ($\text{pM} = 24.5$ and 22.1 respectively), probably due to the chelation and a slightly lower pK_a value (~ 7.4).⁴⁴ In contrast to the glutathione complex, Sb^{3+} coordinates to only the two thiolate groups of the cysteine residues and to one oxygen from a water molecule (Figure 6A). Strong H-bonding between the bound water molecule and the carboxyl oxygen stabilizes the $\text{Sb}(\text{TS}_2)$ structure. Similar to the coordination of $\text{Sb}^{3+}/\text{As}^{3+}$ in the ArsA ATPase, the $\text{Sb}(\text{TS}_2)$ complex can be regarded as an intermediate, and the coordination of a non-protein/peptide ligand may allow it to be more readily replaced by other donor atoms (e.g., thiols). Indeed, both NMR and ESI-MS experiments have confirmed that a ternary complex is formed upon addition of *N*-acetyl-cysteine and glutathione, suggesting that the initial $(\text{H}_2\text{O})\text{Sb}(\text{TS}_2)$ complex changes to $(\text{L})\text{Sb}(\text{TS}_2)$, where L is glutathione or possibly even an enzyme.

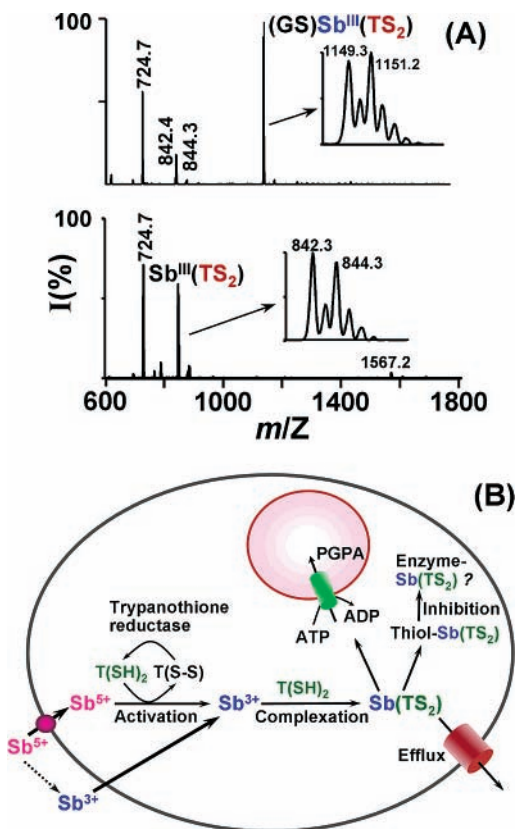


FIGURE 7. (A) ESI-MS spectra of $\text{Sb}(\text{TS}_2)$ (bottom) and $\text{Sb}(\text{TS}_2)$ after addition of glutathione (top) and (B) the proposed molecular mechanism of action of antimonial compounds against *Leishmania*: uptake of Sb^{5+} into parasites; intracellular reduction or activation of Sb^{5+} to Sb^{3+} ; binding of Sb^{3+} to $\text{T}(\text{SH})_2$ followed by enzyme targeting or being pumped out by an ATP-coupled transporter. Adapted from ref 36.

The structure of Sb^{3+} with ArsA ATPase has recently been solved by X-ray crystallography.⁴⁵ This has considerably improved our understanding of the active extrusion of metals, a common mechanism underlying detoxification of heavy metals, drugs, and antibiotics in bacteria, protozoa, and mammals. In *E. coli*, the ArsAB pump, which consists of a soluble ATPase and a membrane channel (ArsB), provides resistance to both arsenite (As^{3+}) and antimonite (Sb^{3+}). The ArsA ATPase is composed of homologous N-terminal (A1) and C-terminal (A2) halves (Figure 6B), both of which have nucleotide binding domains (NBD). NBDs are located at the opposite end of the molecule with respect to the allosteric site. One interesting characteristic of the ATPase is that it is activated upon the binding of Sb^{3+} or As^{3+} , the same ion(s) transported by the ArsAB pump. Surprisingly, a novel trinuclear Sb^{3+} cluster was found to be located at the interface between the two halves of the protein complex (Figure 6B,C). Each of the three Sb^{3+} coordinates to three donor atoms, two of them from the protein residues with one donor atom (ligand) from each domain and one from a nonprotein ligand (Cl^-). Sb^{3+} coordinates to either thiolates or nitrogen groups, for example, Sb_1 to Cys113 (A1) and Cys422 (A2) and Sb_2 to Cys172 (A1) and His453 (A2), or nitrogen- and oxygen-containing groups, for

example, His148 (A1) and Ser420 (A2). The binding of Sb^{3+} (or As^{3+}) brings together the two domains of the enzyme. Similar to the $(\text{H}_2\text{O})\text{Sb}(\text{TS}_2)$ complex, the coordination of the nonprotein ligand (e.g., Cl^-) may allow the $\text{Sb}^{3+}/\text{As}^{3+}$ to be more readily replaced by other thiolates, facilitating their transport.

Despite the fact that Sb^{3+} binds strongly to thiolate sulfurs, these complexes are kinetically labile toward thiolate ligands such as glutathione and trypanothione. The rate of exchange of trypanothione or glutathione with Sb^{3+} is pH dependent, being slower at lower pH values ($5\text{--}10\text{ s}^{-1}$ at $\text{pH} \approx 4$) and considerably faster at $\text{pH} 7$ ($>500\text{ s}^{-1}$ at $\text{pH} \geq 7.4$), as demonstrated by NMR measurements.³⁶ Importantly, exchange between the free and bound forms in the ternary complex $(\text{Cys})\text{Sb}(\text{TS}_2)$ was also observed. Similar types of metal ion exchange among thiolate sulfurs have been noted for other low molecular mass ligands and proteins. Therefore, trypanothione may act as a chaperone, delivering Sb^{3+} via thiolate exchange to target proteins and enzymes within the cell.

Modes of Action of Antimonial Compounds. Upon uptake into cells, Sb^{5+} -containing compounds are reduced or activated to Sb^{3+} either enzymatically or nonenzymatically. Sb^{3+} interferes with trypanothione metabolism in drug-sensitive *Leishmania* parasites and forms a complex with either glutathione⁴³ or trypanothione.³⁶ It may even form a ternary complex between Sb^{3+} , $\text{T}(\text{SH})_2$, and a monothiol ligand, for example, GSH ($(\text{GS})\text{Sb}(\text{TS}_2)$). Complexed Sb^{3+} may then inhibit enzymes such as trypanothione reductase. Simultaneously, Sb^{3+} may also be extruded by the As pump, although direct evidence of cotransport of antimony and thiols is needed to verify this hypothesis (Figure 7B).

4. Concluding Remarks

Recent structural studies of bismuth complexes indicate that Bi^{3+} has a variable coordination number, has an irregular coordination geometry, and is strongly acidic. The polymeric species such as $[\text{Bi}(\text{cit})_2\text{Bi}]_{\infty}^{2n-}$ appear to be the predominant forms of the Bi^{3+} citrate antiulcer drugs. Possible target sites for bismuth in proteins and enzymes are likely to include both ferric iron sites (e.g., both O and N ligands in transferrin or lactoferrin) and zinc and nickel sites (e.g., metallothionein and Hpn). Inhibition of (metallo)enzymes by bismuth may play an important role in the antibactericidal activity of bismuth-containing drugs, and the inhibition is mainly ascribed to its binding to the key cysteine residue(s) within the enzyme.

The relatively nontoxic Sb^{5+} may act as a prodrug, being activated or reduced at or near the site of action both enzymatically and nonenzymatically. Both $\text{Sb}^{\text{III}}(\text{TS}_2)$ and $\text{Sb}^{\text{III}}\text{--ArsA}$ ATPase complexes could act as intracellular intermediates, and labile water or chloride ligands can readily be replaced by a thiolate sulfur (e.g., cysteine) from another molecule, resulting in the formation of a ternary complex. The facile exchange of $\text{Sb}^{3+}\text{--thiolate}$ bonds may be crucial for its transport within parasites and, more

importantly, could be a common feature for metal trafficking among different molecules in cells. Newly developed techniques (e.g., metalloproteomics) should help to establish the molecular mechanisms underlying the antimicrobial activities of bismuth and antimony in a more comprehensive and efficient way and will aid the design of better metallodrugs and novel agents for other therapeutic purposes.

We are grateful to the many research fellows and colleagues who have worked on the topics discussed here. Much of this Account is based on research that has been carried out with the generous support from the Research Grants Council of Hong Kong, Area of Excellence Scheme of UGC (Hong Kong), National Science Foundation of China, the University of Hong Kong (UGC), and Livzon Pharmaceutical Ltd. We thank Dr. Rory Watt for critical comments and his help for the preparation of this paper.

References

- Guo, Z.; Sadler, P. J. *Metals in Medicine*. *Angew. Chem., Int. Ed.* **1999**, *38*, 1512–1531.
- Suerbaum, S.; Michetti, P. *Helicobacter pylori* infection. *N. Engl. J. Med.* **2002**, *347*, 1175–1186.
- Yan, S.; Jin, L.; Sun, H. Antimony in medicine. in *Metallotherapeutic Drugs and Metal-Based Diagnostic Agents: The Use of Metals in Medicine*; Gielen, M., Tiekink, E. R. T., Eds.; John Wiley & Sons: Chichester, U.K., 2005; pp 441–461.
- Sadler, P. J.; Li, H.; Sun, H. Coordination chemistry of metals in medicine: Target sites for bismuth. *Coord. Chem. Rev.* **1999**, *185–186*, 689–709.
- Andrews, P. C.; Deacon, G. B.; Frosyth, C. M.; Junk, P. C.; Kumar, I.; Maguire, M. Towards a structural understanding of the anti-ulcer and anti-gastritis drug bismuth subsalicylate. *Angew. Chem., Int. Ed.* **2006**, *45*, 5638–5642.
- Sun, H.; Zhang, L.; Szeto, K. Y. Bismuth in medicine. *Met. Ions Biol. Syst.* **2004**, *41*, 333–378.
- Asato, E.; Katsura, K.; Mikuriya, M.; Turpeinen, U.; Mutikainen, I.; Reedijk, J. Synthesis, structure, and spectroscopic properties of bismuth citrate compounds and the bismuth-containing ulcer-healing agent colloidal bismuth citrate (CBS). 4. Crystal structure and solution behavior of a unique dodecanuclear cluster. *Inorg. Chem.* **1995**, *34*, 2447–2454.
- Li, W.; Jin, L.; Zhu, N.; Hou, X.; Deng, F.; Sun, H. Structure of colloidal bismuth subcitrate (CBS) in dilute HCl: Unique assembly of bismuth citrate dinuclear units $[\text{Bi}(\text{cit})_2\text{Bi}]^{2-}$. *J. Am. Chem. Soc.* **2003**, *125*, 12408–12409.
- Barrie, P. J.; Djuran, M. I.; Mazid, M. A.; McPartlin, M.; Sadler, P. J.; Scowen, I. J.; Sun, H. Solid-state carbon-13 nuclear magnetic resonance investigation of bismuth citrate complexes and crystal structure of $\text{Na}_2[\text{Bi}_2(\text{cit})_2] \cdot 7\text{H}_2\text{O}$. *J. Chem. Soc., Dalton Trans.* **1996**, 2417–2422.
- Chen, R.; So, M.H.; Yang, J.; Deng, F.; Che, C. M.; Sun, H. Fabrication of bismuth nanotube arrays from bismuth citrate. *Chem. Commun.* **2006**, 2265–2267.
- Lee, M. B.; Gilbert, H. M. Current approaches to Leishmaniasis. *Infect. Med.* **1999**, *16*, 37–45.
- Roberts, W. I.; McMurray, W. J.; Rainey, P. M. Characterization of the antimonial antileishmanial agent meglumine antimonate (glucantime). *Antimicrob. Agents Chemother.* **1998**, *42*, 1076–1082.
- Hollemann, A. F.; Wiberg, E. *Lehrbuch der Anorganischen Chemie*; Walter de Gruyter: Berlin, 1985; p 688.
- Aisen, P. Transferrin, the transferrin receptor, and the uptake of iron by cells. *Met. Ions Biol. Syst.* **1998**, *35*, 585–631.
- Sun, H.; Li, H.; Sadler, P. J. Transferrin as a metal ion mediator. *Chem. Rev.* **1999**, *99*, 2817–2842.
- Aisen, P.; Adela, L. Lactoferrin and transferrin. Comparative study. *Biochim. Biophys. Acta* **1972**, *257*, 314–323.
- Zhang, L.; Szeto, K. Y.; Wong, W. B.; Loh, T. T.; Sadler, P. J.; Sun, H. Interactions of bismuth with human lactoferrin and recognition of the Bi^{III} -lactoferrin complex by intestinal cells. *Biochemistry* **2001**, *40*, 13281–13287.
- Sun, H.; Li, H.; Mason, A. B.; Woodworth, R. C.; Sadler, P. J. Competitive binding of bismuth to transferrin and albumin in aqueous solution and in blood plasma. *J. Biol. Chem.* **2001**, *276*, 8829–8835.
- Slikkerveer, A.; de Wolff, F. A. Pharmacokinetics and toxicity of bismuth compounds. *Med. Toxicol. Adverse Drug Exp.* **1989**, *4*, 303–323.
- Rao, N.; Feldman, S. Disposition of bismuth in the rat. I. red blood cell and plasma protein binding. *Pharm. Res.* **1990**, *7*, 188–191.
- Sun, H.; Szeto, K. Y. Binding of bismuth to serum proteins: implication for targets of $\text{Bi}(\text{III})$ in blood plasma. *J. Inorg. Biochem.* **2003**, *94*, 114–120.
- Blaser, M. J. Hypotheses on the pathogenesis and natural history of *Helicobacter pylori*-induced inflammation. *Gastroenterology* **1992**, *102*, 720–727.
- Lambert, J. R.; Midolo, P. The action of bismuth in the treatment of *Helicobacter pylori* infection. *Aliment. Pharmacol. Ther.* **1997**, *11* (Suppl), 27–33.
- Jin, L.; Szeto, K. Y.; Zhang, L.; Du, W. H.; Sun, H. Inhibition of alcohol dehydrogenase by bismuth. *J. Inorg. Biochem.* **2004**, *98*, 1331–1337.
- Asato, E.; Kamamuta, K.; Akamine, Y.; Fukami, T.; Nukada, R.; Mikuriya, M.; Deguchi, S.; Yokota, Y. Bismuth(III) complexes of 2-mercaptoethanol: Preparation, structural and spectroscopic characterization, antibactericidal activity toward *Helicobacter pylori*, and inhibitory effect towards *H. pylori*-produced urease. *Bull. Chem. Soc. Jpn.* **1997**, *70*, 639–648.
- Zhang, L.; Mulrooney, S. B.; Fung, A. F. K.; Zeng, Y.; Ko, B. B. C.; Hausinger, R. P.; Sun, H. Inhibition of urease by bismuth(III): Implication for the mechanism of action of bismuth drugs. *BioMetals* **2006**, *19*, 503–511.
- Ge, R.; Watt, R. M.; Sun, X.; Tanner, J. A.; He, Q.-Y.; Huang, J.-D.; Sun, H. Expression and characterization of a histidine-rich protein: potential for Ni^{2+} storage in *Helicobacter pylori*. *Biochem. J.* **2006**, *393*, 285–293.
- Ge, R.; Zhang, Y.; Sun, X.; Watt, R. M.; He, Q.-Y.; Huang, J.-D.; Wilcox, D. E.; Sun, H. Thermodynamic and kinetic aspects of metal binding to the histidine-rich protein, Hpn. *J. Am. Chem. Soc.* **2006**, *128*, 11330–11331.
- Kluefers, P.; Mayer, P. Polyol-metal-komplexe. 27. Bisdiolato antimonates(III) with guanosine as the diol. *Z. Anorg. Allg. Chem.* **1997**, *623*, 1496–1498.
- Demicheli, C.; Frezard, F.; Lecouvey, M.; Garnier-Suillerot, A. Antimony(V) complex formation with adenine nucleosides in aqueous solution. *Biochim. Biophys. Acta* **2002**, *1570*, 192–198.
- Hansen, H. R.; Pergantis, S. A. Mass spectrometric identification and characterization of antimony complexes with ribose-containing biomolecules and an RNA oligomer. *Anal. Bioanal. Chem.* **2006**, *385*, 821–833.
- Chai, Y.; Yan, S.; Wong, I. L. K.; Chow, L. M. C.; Sun, H. Complexation of antimony (Sb^{V}) with guanosine 5'-monophosphate and guanosine 5'-diphospho-d-mannose: Formation of both mono- and bis-adducts. *J. Inorg. Biochem.* **2005**, *99*, 2257–2263.
- Shaked-Mishan, P.; Ulrich, N.; Ephros, M.; Zilberstein, D. Novel intracellular Sb^{V} reducing activity correlates with antimony susceptibility in *Leishmania donovani*. *J. Biol. Chem.* **2001**, *276*, 3971–3976.
- Frezard, F.; Demicheli, C.; Ferreira, C. S.; Costa, M. A. P. Glutathione-induced conversion of pentavalent antimony to trivalent antimony in meglumine antimonate. *Antimicrob. Agents Chemother.* **2001**, *45*, 913–916.
- Fairlamb, A. H.; Cerami, A. Metabolism and functions of trypanothione in the Kinetoplastida. *Annu. Rev. Microbiol.* **1992**, *46*, 695–729.
- Yan, S.; Li, F.; Ding, K.; Sun, H. Reduction of pentavalent antimony by trypanothione and formation of a binary and ternary complex of antimony(III) and trypanothione. *J. Biol. Inorg. Chem.* **2003**, *8*, 689–697.
- Yan, S.; Wong, I. L. K.; Chow, L. M. C.; Sun, H. Rapid reduction of pentavalent antimony by trypanothione: potential relevance to antimonial activation. *Chem. Commun.* **2003**, 266–267.
- Wyllie, S.; Cunningham, M. L.; Fairlamb, A. H. Dual action of antimonial drugs on thiol redox metabolism in the human pathogen *Leishmania donovani*. *J. Biol. Chem.* **2004**, *279*, 3995–39932.
- Glaser, T. A.; Baatz, J. E.; Kreishman, G. P.; Mukkada, A. J. pH homeostasis in *Leishmania donovani* amastigotes and promastigotes. *Proc. Natl. Acad. Sci. U.S.A.* **1988**, *85*, 7602–7606.
- Brochu, C.; Wang, J. Y.; Roy, G.; Messier, N.; Wang, X. Y.; Saravia, N. G.; Ouellette, M. Antimony uptake systems in the protozoan parasite *Leishmania* and accumulation differences in antimony-resistant parasites. *Antimicrob. Agents Chemother.* **2003**, *47*, 3073–3079.
- Zhou, Y.; Messier, N.; Ouellette, M.; Rosen, B. P.; Zilberstein, D. *Leishmania major* LmACR2 is a pentavalent antimony reductase that confers sensitivity to the drug pentostam. *J. Biol. Chem.* **2004**, *279*, 37445–37451.

- (42) Denton, H.; McGregor, J. C.; Coombs, G. H. Reduction of anti-leishmanial pentavalent antimonial drugs by a parasite-specific thiol-dependent reductase, TDR1. *Biochem. J.* **2004**, *381*, 405–412.
- (43) Sun, H.; Yan, S.; Cheng, W. S. Interaction of antimony tartrate with the tripeptide glutathione implication for its mode of action. *Eur. J. Biochem.* **2000**, *267*, 5450–5457.
- (44) Yan, S.; Ding, K.; Zhang, L.; Sun, H. Complexation of antimony(III) to trypanothione. *Angew. Chem., Int. Ed.* **2000**, *39*, 4260–4262.
- (45) Zhou, T.; Radaev, S.; Rosen, B. P.; Gatti, D. L. Structure of the ArsA ATPase: The catalytic subunit of a heavy metal resistance pump. *EMBO J.* **2000**, *19*, 4838–4845.

AR60001B